ChemPubSoc Europe

DOI: 10.1002/cmdc.201400037

Chiral Resolution and Pharmacological Characterization of the Enantiomers of the Hsp90 Inhibitor 2-Amino-7-[4-fluoro-2-(3-pyridyl)phenyl]-4-methyl-7,8-dihydro-6*H*-quinazolin-5-one Oxime

Raffaella Amici,*[a, f] Chiara Bigogno,[b, g] Roberto Boggio,[a, h] Andrea Colombo,[b, i] Stephen M. Courtney,[c] Roberto Dal Zuffo,[d, f] Giulio Dondio,[b, g] Fulvia Fusar,[d, f] Stefania Gagliardi,[b, j] Saverio Minucci,[e] Marco Molteni,[b, k] Christian A. G. N. Montalbetti,[c, l] Annalisa Mortoni,[b, m] Mario Varasi,[d, f] Stefania Vultaggio,[d, f] and Ciro Mercurio[d, f]

Heat-shock protein 90 (Hsp90) is a molecular chaperone involved in the stabilization of key oncogenic signaling proteins, and therefore, inhibition of Hsp90 represents a new strategy in cancer therapy. 2-Amino-7-[4-fluoro-2-(3-pyridyl)phenyl]-4-methyl-7,8-dihydro-6*H*-quinazolin-5-one oxime is a racemic Hsp90 inhibitor that targets the N-terminal adenosine triphosphatase site. We developed a method to resolve the enantiomers and evaluated their inhibitory activity on Hsp90 and the consequent antitumor effects. The (*S*) stereoisomer emerged as a potent Hsp90 inhibitor in biochemical and cellular assays. In addition, this enantiomer exhibited high oral bioavailability in mice and excellent antitumor activity in two different human cancer xenograft models.

Introduction

Heat-shock protein 90 (Hsp90) is an adenosine triphosphate (ATP)-dependent molecular chaperone involved in the conformational maturation of several client proteins implicated in multiple and diverse cellular functions.[1] The Hsp90 protein consists of three distinct domains:[2] the N-terminal ATP binding domain, the middle domain involved in the ATPase cycle and in the binding with co-chaperone and client proteins, and the C-terminal domain, with a role in a homodimerization process and in the allosteric control over both substrates and N-terminal pocket.[3]

The function of Hsp90 is regulated by a concerted mechanism, defined as the chaperone cycle; it involves the nucleotide domain pocket in the N-terminal region of the protein, as well the middle region and the C-terminal nucleotide binding pocket.[4–6] An additional level of regulation of Hsp90 function is represented by both the interaction of Hsp90 with diverse co-chaperones and by several post-translational modifications such as acetylation, nitrosylation, and phosphorylation.[6] The occupancy of both the N-terminal ATP binding site and the C-terminal pocket by high affinity ligands, which inhibit Hsp90,

[a] *Dr. R. Amici, Dr. R. Boggio*
Genextra Group, Congenia s.r.l., Via Adamello 16, 20139 Milan (Italy)
E-mail: raffaella.amici@ieo.eu

[b] *Dr. C. Bigogno, Dr. A. Colombo, Dr. G. Dondio, Dr. S. Gagliardi, Dr. M. Molteni, Dr. A. Mortoni*
NiKem Research s.r.l., Via Zambeletti 25, 20021 Baranzate (Italy)

[c] *Dr. S. M. Courtney, Dr. C. A. G. N. Montalbetti*
Evotec, 114 Milton Park, Abingdon, Oxfordshire, OX10 4SA (UK)

[d] *Dr. R. Dal Zuffo, Dr. F. Fusar, Dr. M. Varasi, Dr. S. Vultaggio, Dr. C. Mercurio*
Genextra Group, DAC s.r.l., Via Adamello 16, 20139 Milan (Italy)

[e] *Prof. Dr. S. Minucci*
IEO–European Institute of Oncology, Via Adamello 16, 20139 Milan (Italy)
and
Department of Life Sciences, University of Milan
Via Celoria 26, 20133 Milan (Italy)

[f] *Dr. R. Amici, Dr. R. Dal Zuffo, Dr. F. Fusar, Dr. M. Varasi, Dr. S. Vultaggio, Dr. C. Mercurio*
Current address: Drug Discovery Program
Department of Experimental Oncology
IEO-European Institute of Oncology, Via Adamello 16, 20139 Milan (Italy)

[g] *Dr. C. Bigogno, Dr. G. Dondio*
Current address: Aphad s.r.l.
Via della Resistenza 65, 20090 Buccinasco (MI) (Italy)

[h] *Dr. R. Boggio*
Current address: IRBM Promidis s.r.l.
Via Pontina km 30, 600, 00040 Pomezia (RM) (Italy)

[i] *Dr. A. Colombo*
Current address: Teva Pharmaceuticals Fine Chemicals
Strada Statale Briantea, 23892 Bulciago (Italy)

[j] *Dr. S. Gagliardi*
Current address: Flamma S.p.A.
Via Bedeschi 22, 24040 Chignolo d'Isola (BG) (Italy)

[k] *Dr. M. Molteni*
Current address: Chorisis s.r.l.
Via R. Lepetit 34, 21040 Gerenzano (VA) (Italy)

[l] *Dr. C. A. G. N. Montalbetti*
Current address: Inventiva, 50 rue de Dijon, 21121 Daix (France)

[m] *Dr. A. Mortoni*
Current address: CISI S.C.R.L.
Via G. Fantoli 16/15, 20138 Milan (Italy)

 © 2014 Wiley-VCH Verlag GmbH & Co. KGaA, Weinheim

prevents the Hsp90 client proteins from achieving their mature functional conformation.

Additional strategies to inhibit Hsp90 have also been identified[7] and pursued by targeting the co-chaperone/Hsp90 interaction and specifically by targeting the Cdc37/Hsp90 interaction[8] and interaction between Hsp90 and the co-chaperone containing a tetratricopeptide region[9] as well as targeting client/Hsp90 associations.[10,11]

Many of the Hsp90 client proteins are overexpressed and/or mutated in cancer and are directly associated with cancer progression. Among them, we can find ERBB2, CDK4, c-Raf, B-Raf, c-Met, and h-Tert. Consequently, there is no surprise that Hsp90 has an important role in maintaining the activity and stability of key oncogenic signaling proteins.[5] Furthermore, elevated Hsp90 expression has been documented in different tumor types, and a correlation exists between high expression of Hsp90 and poor disease prognosis.[12–19] The inhibition of Hsp90 and the loss of its chaperone function leads client proteins to be degraded by the ubiquitin proteasome pathways, which consequently disrupted their oncogenic function. Given that Hsp90 is involved in the control of a multitude of pathways relevant for cancer progression, its inhibition permits a concerted attack on the unrestricted proliferation and survival of cancer cells, and this leads to cell growth inhibition and apoptosis.

The relevance of Hsp90 as target for cancer therapy has been extensively established and reviewed in the last years.[20–23] Up to now, the vast majority of drug-development efforts have focused on inhibitors binding to the N-terminal ATP binding site, but a second druggable site was identified in the C-terminal domain of Hsp90.[24] To date, no C-terminal inhibitor has advanced into clinical trial. Indeed, all of the 17 clinically evaluated Hsp90 inhibitors belong to the so called N-terminal inhibitors.[25]

With regard to these inhibitors, the natural product geldanamycin was the first reported inhibitor of Hsp90. Since then, several geldanamycin derivatives such as 17-AAG, 17-DMAG, and IPI-504 (Figure 1)[26] have been investigated in preclinical and clinical studies. Furthermore, synthetic small-molecule inhibitors from unrelated chemical classes have been discovered, some of which are currently in clinical trials for the treatment of cancer. The structures of these new agents belong to three main classes: ATP mimetics through an amino-substituted fused heteroaromatic bicyclic ring system, resorcinol analogues, and 2-aminobenzamides.[26] All of them target the N-terminal ATP pocket of Hsp90. Representative examples (Figure 1) are the oral-drug candidates XL-888 (Exelixis, phase I);[27] DEBIO-0932/CUDC-305 (Debiopharm/Curis, phase I);[28] MPC-3100 (Myrexis Inc., phase I);[29] PF-4929113/SNX-5422 (Pfizer, phase I), which is a glycine prodrug of PF-4928473/SNX-2112;[30] BIIB021 (Biogen Idec, phase II);[31] and NVP-HSP990 (Novartis, phase I).[32] Compounds pursued as intravenous agents include NVP-AUY922 (Novartis, phase II),[33] AT13387 (Astex, phase II),[34] STA-9090 (Synta, phase II/III),[35] KW-2478 (Kyowa Hakko Kirin, phase I/II),[36] and PU-H71 (Memorial Sloan-Kettering Cancer Center, phase I).[37] Although some concerns about the safety profile of N-terminal Hsp90 inhibition have been raised, there are currently 38 clinical trials that are ongoing with these molecules. One compound, STA-9090, is in phase III evaluation in patients with non-small-cell lung cancer treated with docetaxel plus or minus ganetespib. Moreover, the very recent clinical data obtained with BIIB021, which indicates both good tolerability and responses consistent with anti-Hsp90 biologic activity, demonstrates that important progress has been made in overcoming some issues previously observed.[25]

With respect to C-terminal inhibitors (Figure 2), clear improvement in the prototypic C-terminal inhibitor novobiocin has been accomplished, and molecules showing interesting in vivo efficacy data in preclinical studies have been identified (KU174 and KU363).[38–41]

Importantly, the C-terminal inhibitors represent an interesting and possibly alternative approach, because these molecules, differently from N-terminal inhibitors, do not induce a prosurvival heat-shock response,[42] and this could increase the effectiveness of the inhibitors as antitumor agents.[43]

As part of our efforts to find new potent Hsp90 inhibitors, we performed a high-throughput biochemical fragment screening campaign. Further optimization of the hits by using a combination of in silico commercial analogue selection and structure-based design led to the identification of compound **1**.[44] This compound, which exhibits good biochemical and cellular activity, has one stereogenic carbon atom; consequently, it corresponds to a racemic mixture of two possible enantiomers. Our further efforts were therefore directed toward the separation of racemic compound **1** and biological characterization of the two enantiomers to investigate the influence of the stereochemistry on the identified Hsp90 inhibitory activity.

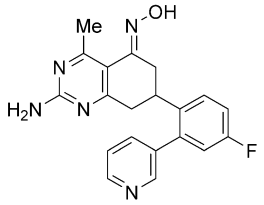

compound **1**

In this study, we report a method to produce the pure enantiomers of compound **1** on both small and large scales. The paper further reports their biological and absorption, distribution, metabolism, and excretion (ADME) characterization, their in vivo pharmacokinetic profile, and in vivo efficacy in xenograft models.

Results and Discussion

Enantiomeric separation and in vitro characterization

For the initial characterization of the enantiomers, we conducted the resolution of racemic mixture **1** by chiral chromatography by using a Daicel Chiralpak AD semipreparative column with a heptane/2-propanol mixture (75:25) containing 0.1%

© 2014 Wiley-VCH Verlag GmbH & Co. KGaA, Weinheim

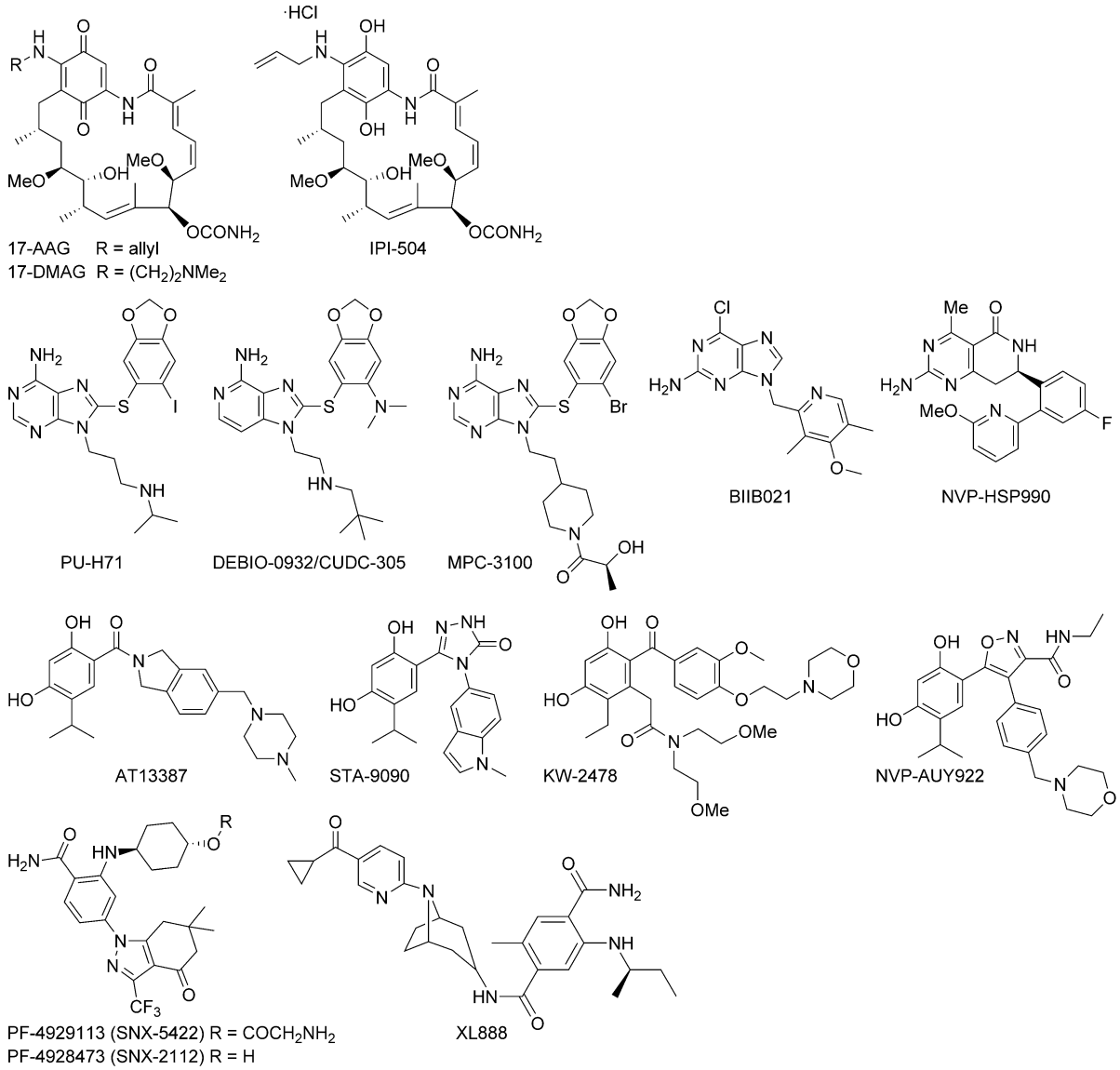

Figure 1. Hsp90 inhibitors in clinical development.

triethylamine as the eluent. The obtained enantiomers were evaluated for their Hsp90 inhibitory activity as well as for their antiproliferative effects in comparison with the racemic mixture. Interestingly, a clear difference in the activity profiles for the distinct enantiomers was observed. As shown in Table 1, stereoisomer **2** exhibited very potent Hsp90 inhibitory activity ($IC_{50} = 19$ nM), which was clearly superior to that of enantiomer **3** and racemate **1**. Similarly and congruently, enantiomer **2** was more potent than enantiomer **3** and racemic mixture **1** in the antiproliferative assay on the two human cancer cell lines A549 and HCT-116.

Table 1. Hsp90 enzyme and antiproliferative activity data for racemate **1** and enantiomers.[a]

Compound	Activity [μM]		
	Enzyme	A549	HCT-116
racemate **1**	0.030 ± 0.001	0.85 ± 0.01	0.85 ± 0.09
enantiomer **2**	0.019 ± 0.001	0.29 ± 0.038	0.42 ± 0.079
enantiomer **3**	1.10 ± 0.04	> 2.5	2.3 ± 0.779

[a] Assays done in replicates ($n \geq 2$); mean values and standard deviations are shown.

We subsequently analyzed the molecular signature of Hsp90 inhibition on HCT-116 cells by following the induction of Hsp70 and the depletion of the well-known Hsp90 client protein c-Raf.[45] Racemate **1** and enantiomers **2** and **3** were tested at concentrations that were 0.2-, 1-, and 5-fold the antiproliferative IC_{50} value on HCT-116 cells. The objective was to find a correlation between the observed antiproliferation effect and Hsp90 inhibition. As reported in Figure 3, all three compounds were able to determine a dose-dependent induction of Hsp70, whereas only racemate **1** and enantiomer **2**, but not enantiomer **3**, were able to induce a down-regulation of c-Raf under

© 2014 Wiley-VCH Verlag GmbH & Co. KGaA, Weinheim

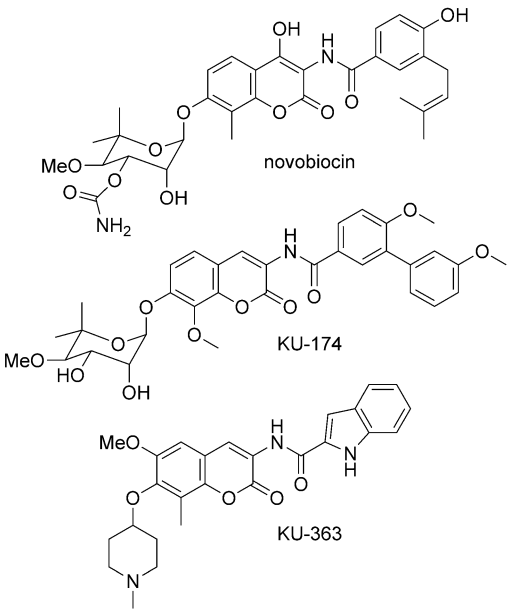

Figure 2. Structures of C-terminal inhibitors.

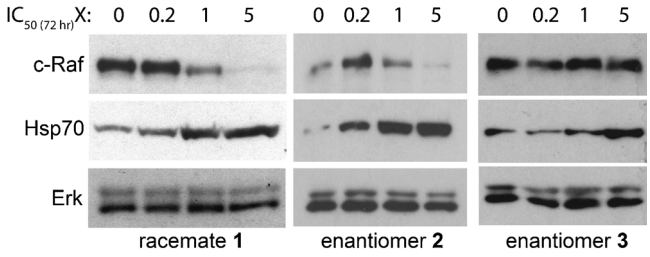

Figure 3. Western blot of racemate **1** and enantiomers **2** and **3** on HCT-116 cell lines. Target modulation at 24 h tested at 0, 0.2, 1, and 5 times the respective cellular IC_{50} value. The expression levels of Erk were used as loading control.

the experimental conditions; this suggested that the antiproliferative effect determined by enantiomer **3** was not directly related to Hsp90 inhibition.

Co-crystallization experiments were conducted on both enantiomers, but the only crystal structure that was obtained in our hands was that of enantiomer **2**, to which an *S* configuration was assigned (PDB code: 3FT8).[44] On the basis of these results, redocking experiments were performed on all four possible conformations of the two enantiomers (i.e., *S* with axial 3-pyridylphenyl, *S* with equatorial 3-pyridylphenyl, and the corresponding *R* conformations). In agreement with the X-ray data, only the *S* equatorial configuration showed favorable interactions with the aromatic cage constituted by Phe138, Tyr139, and Trp162, whereas the *R* equatorial enantiomer was sterically hindered (Figure 4). As shown in the figure, the fluorine atom of the *R* enantiomer in particular shows an unfavorable interaction with the protein.

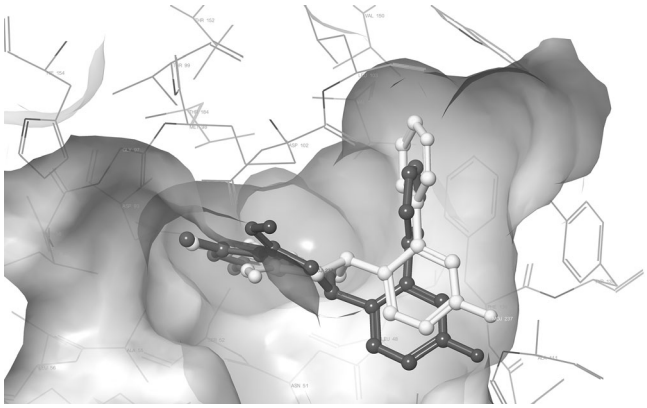

Figure 4. The *S* enantiomer (grey) and *R* enantiomer (black) docked into the N-terminal ATP binding site of Hsp90.

As the next step, enantiomers **2** and **3** were evaluated in a series of ADME experiments. The compounds were incubated with mouse and human microsomes at 37 °C for 30 min, and the percentage of unmetabolized product was assessed by LC–MS/MS. As illustrated in Table 2, enantiomers **2** and **3** had similar stability in mouse and human microsomes. The derivatives showed low aqueous solubility at neutral pH and acceptable solubility at pH 4. The protein binding was 97 and 95% for enantiomers **2** and **3**, respectively. Moreover, inhibition of key drug-metabolizing cytochromes P450 (CYPs) was assessed, which is relevant both in the pharmacokinetics of xenobiotics and in adverse drug–drug interactions.[46] For this purpose, the compounds were incubated at final concentrations of 1 μM with the cytochrome isozymes CYP1A2, CYP2C9, CYP2D6, and CYP3A4 and the specific substrates for 15–45 min. The percentages of inhibition of the cytochrome isoenzymes are summarized in Table 2. Similar inhibition (≈24%) on CYP2C9 was observed for both enantiomers. Interestingly, enantiomer **2** showed only minor interference (<5%) on the CYP1A2, CYP2D6, and CYP3A4 cytochromes. In contrast, enantiomer **3** inhibited the enzyme activity of cytochromes CYP3A4 and CYP2D6 by ~30%.

On the basis of the promising in vitro data, we decided to evaluate the compounds in vivo. It was therefore necessary to establish a method to produce quantities of the chiral derivatives sufficient for the in vivo evaluations. The use of a variety

Table 2. In vitro ADME parameters of enantiomers **2** and **3**.[a]

Compd	Microsomal stability [%]		Solubility [μM]		PPB [%]	Cytochrome P450 inhibition at 1 μM [%]			
	Mouse	Human	pH 7.4	pH 4		1A2	2C9	2D6	3A4
2	23	38	34	208	97	<5	24	<5	<5
3	34	38	29	181	95	7.6	24	32	32

[a] Assays done in replicates ($n \geq 2$); mean values are shown, and standard deviations are <30% of the mean.

© 2014 Wiley-VCH Verlag GmbH & Co. KGaA, Weinheim

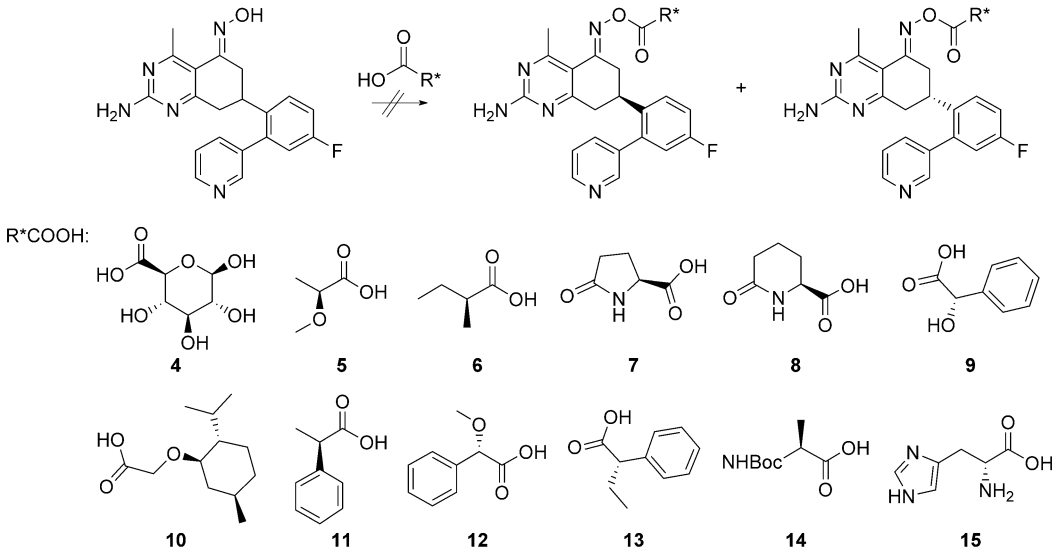

Scheme 1. *Reagents and conditions*: DMF, EDC, HOBT, TEA, R*COOH at room temperature or with microwave heating. Boc = *tert*-butoxycarbonyl.

of chiral auxiliaries in the synthesis of racemate **1** did not provide satisfactory results. Thus, the oxime group of compound **1** was selected as a functionalization site, and various commercial chiral acids were used for the synthesis of the corresponding oxime esters (Scheme 1). The syntheses were performed with hydroxybenzotriazole (HOBt), 1-ethyl-3-(3-dimethylaminopropyl)-carbodiimide (EDC), and triethylamine (TEA) in DMF at room temperature or by heating under microwave irradiation if necessary. With the exception of acids **4**, **9**, **12**, and **15**, all other acids afforded the desired esters; however, separation of the diastereomers was not possible.

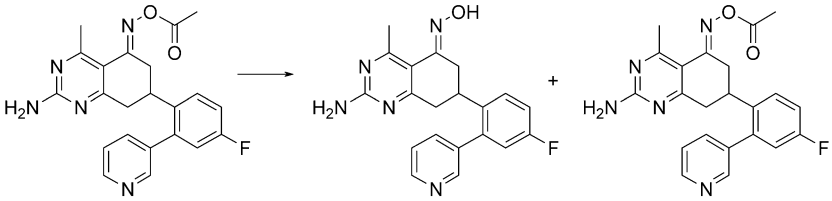

a) Lipase from *Candida antarctica*: conversion ~20%, 76:24 *S*/*R* in 14 days
b) Amano lipase AK from *Pseudomonas fluorescens*: no reaction
c) Lipase from *Candida cylindracea*: no reaction
d) Esterase immobilized on Eupergit C from hog liver: no enantioselection
e) Protease from *Bacillus licheniformis*: no enantioselection
f) Porcine pancreatic lipase: no reaction

Scheme 2. *Reagents and conditions*: Enzyme, EtOH, room temperature.

The use of enzymatic methods was then evaluated for resolving racemate **1**. Lipases are extensively used to catalyze stereoselective esterifications, transesterifications, and hydrolyses in non-aqueous media.[47,48] Oxime esters show intermediate reactivity as irreversible acyl-transfer agents for lipase catalysis and, therefore, can be used under mild conditions in enzymatic transesterification reactions.[49–52] As a first attempt, enantioselective acetylation of compound **1** was undertaken. The reaction was performed with vinyl acetate in ethanol by using amano lipase AK from *Pseudomonas fluorescens*; however, no desired products were obtained. Enantioselective hydrolysis of acetylated derivative **1** was then considered. Racemate **1** was treated with acetyl chloride and TEA in DMF at room temperature overnight. The resultant acetate was then treated with several enzymes in ethanol at room temperature (Scheme 2).

The most promising results were obtained by using lipase immobilized from *Candida antarctica*, which led to low conversion into the hydrolyzed free oxime (20% by UPLC analysis) with *S*/*R* = 76:24 (HPLC analysis on a chiral stationary phase). Optimal conditions were found with the lipase acrylic resin from *C. antarctica* in THF with butanol at 30 °C over 36 h (Scheme 3). Under these conditions, hydrolysis of the *O*-acetyl oxime moiety of compound **1** resulted in 50% conversion into the free oxime. The enantiomeric ratio was *S*/*R* = 9:1, and the remaining *O*-acetylated oxime had an enantiomeric ratio of *S*/*R* = 7:93. The free oxime was subsequently re-acetylated and triturated with methanol. Both the filtered solid and the mother liquors were analyzed by HPLC on a chiral stationary phase. Surprisingly, the mother liquors contained 99% of the *S* enantiomer, and the solid contained the acetyl oxime with *S*/*R* = 8:2. It is well known that nonracemic enantiomeric mixtures can form homochiral and heterochiral aggregates in melt or suspension during adsorption or crystallization. These diastereomeric associations determine the distribution of the

© 2014 Wiley-VCH Verlag GmbH & Co. KGaA, Weinheim

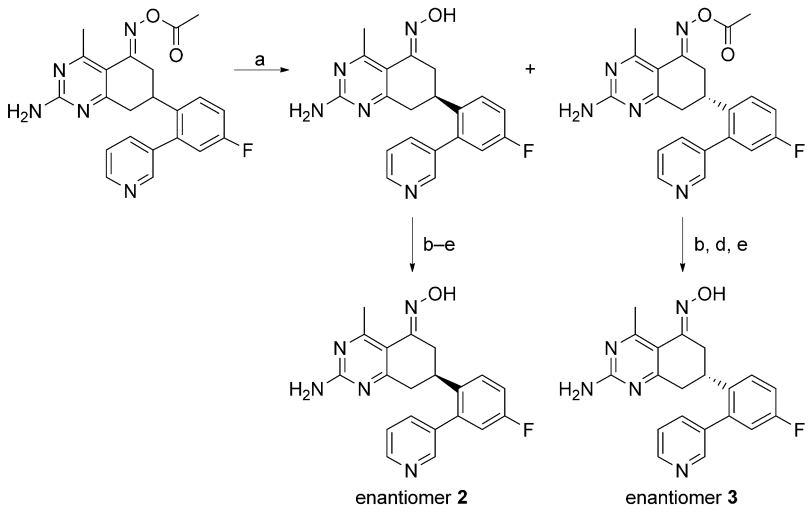

Scheme 3. *Reagents and conditions*: a) Lipase acrylic resin from *C. antarctica*, THF/*n*BuOH, 30 °C; b) separation by flash chromatography; c) CH_3COCl, TEA, DMF, room temperature; d) trituration in MeOH; e) NaOH, MeOH, room temperature.

enantiomers between the solid phase and other phases.[53,54] The distribution depends on the stability order of the homo- and heterochiral aggregates (conglomerates or racemate formation). These aggregates are diastereomeric, and they can be differentiated under achiral conditions. The (*S*)-acetyl oxime from the mother liquors was then treated with NaOH to obtain free enantiomer **2** (enantiomeric purity $S > 98\%$). The originally obtained *O*-acetylated oxime with $S/R = 7{:}93$ was converted following the same procedure into the (*R*)-acetylated enantiomer (enantiomeric purity of 100%). Similar results in terms of enantiomeric purity and recovered yield were obtained by treating the *O*-acetyl oximes in a second run with lipase acrylic resin from *C. antarctica* under the previously described conditions. However, it is evident that this second enzymatic run is more expensive and time consuming than simple trituration with methanol.

Following isolation of sufficient quantities of the enantiomers, the in vivo pharmacokinetic behavior was determined. The compounds were administrated to CD-1 mice in a single intravenous (IV) dose of 5 mg kg^{-1} or an oral dose of 15 mg kg^{-1}. The main plasma pharmacokinetic parameters are reported in the Table 3. Following IV administration, enantiomer **2** showed a systemic plasma clearance of 32 mL min^{-1} kg^{-1}, which is lower than hepatic blood flow in mice (86 mL min^{-1} kg^{-1}),[55] an estimated elimination half-life of 71 min, and a volume of distribution that was three times higher than mice total body water; this is suggestive of good tissue distribution. Following oral administration, enantiomer **2** was rapidly absorbed with $t_{max} = 15$ min and showed high oral bioavailability (95%). Enantiomer **3**, however, exhibited a higher clearance rate (56.4 vs. 32 mL min^{-1} kg^{-1}) and significantly lower oral exposure and bioavailability (33.7 vs. 95%) than enantiomer **2**.

In vivo efficacy

The two enantiomers were then submitted to an in vivo efficacy experiment in an established human HCT-116 xenograft model. Human cancer cells HCT-116 (5×10^6) were injected subcutaneously in the flank of female CD-1 nude mice, and treatment was initiated once the tumors reached a volume of 100 mm^3. Enantiomer **2** was orally administered at doses of 30, 50, and 100 mg kg^{-1} for five days per week for 16 days, whereas enantiomer **3** was orally administered only at the highest dose of 100 mg kg^{-1}. As shown in Figure 5a, oral administration of enantiomer **2** resulted in a significant dose-dependent decrease in the tumor volume relative to the control group. Specifically, the calculated tumor/control ratio (T/C) at doses of 30, 50, and 100 mg kg^{-1} were 0.42, 0.37, and 0.3, respectively, with *p* values of 0.01, 0.004, and 0.0003. Importantly, enantiomer **3** was less active than enantiomer **2** at the dose of 100 mg kg^{-1} with a calculated T/C of 0.69. No significant body weight differences among the groups of mice and no signs of evident toxicity were observed during treatment.

Four hours after the end of the treatment, three tumors were randomly taken both from the group of control mice and from the group of mice treated with compound **2** at doses of 30, 50, and 100 mg kg^{-1}. Western blotting of the lysates of the recovered tumors showed that enantiomer **2** effectively induced the degradation of the Hsp90 client protein as c-Raf in the majority of the analyzed samples (Figure 5b). Concurrently, a significant inhibition of mitogen-activated protein kinase (MAPK), as measured by decreased phosphorylation levels of Erk, was observed mainly at doses of 50 and 100 mg kg^{-1}.

Enantiomer **2** was then evaluated in a non-small-cell lung (NSCL) xenograft model as a single agent and in combination

Table 3. Pharmacokinetic data of enantiomers **2** and **3** in mice.[a]

Compd	C_{max}(IV) [ng mL^{-1}]	AUC(IV)$_{0-\infty}$ [min ng mL^{-1}]	$t_{1/2}$ [min]	Cl [mL min^{-1} kg^{-1}]	V_{ss} [L kg^{-1}]	C_{max}(OS) [ng mL^{-1}]	t_{max} [min]	AUC(OS)$_{0-\infty}$ [min ng mL^{-1}]	*F* [%]
2	3979	156429	71	32	2.1	1964	15	447063	95
3	4756	88680	163	56.4	2.45	858	15	89836	33.7

[a] C_{max}: maximum concentration; AUC: area under curve; $t_{1/2}$: half-life; Cl: clearance; V_{ss}: steady-state volume of distribution; *F*: bioavailability.

© 2014 Wiley-VCH Verlag GmbH & Co. KGaA, Weinheim

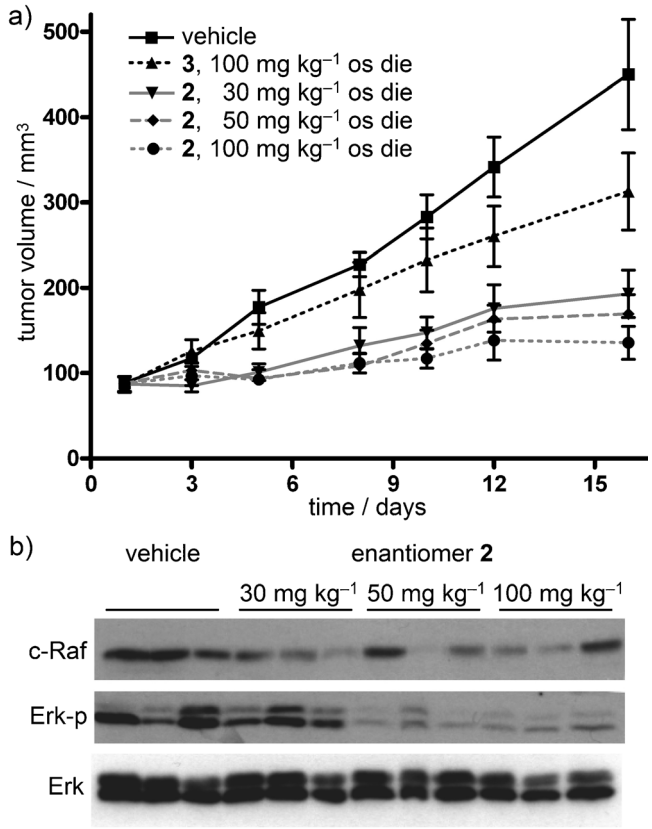

Figure 5. a) Antitumor activity of **2** and **3** against HCT-116 human tumor xenografts implanted in mice, expressed as the mean tumor volume (expressed as mm^3) ± standard error of the mean (SEM). Enantiomer **2** was orally administered at doses of 30, 50, and 100 mg kg^{-1} for five days per week for 16 days, whereas enantiomer **3** was orally administered only at the highest dose of 100 mg kg^{-1} (os die: per os daily). b) Analysis by western blot of c-Raf, phosphorylated Erk (Erk-p), and Erk of the lysate of HCT-116 xenograft tumor at the end of treatment.

with paclitaxel. NSCL human cancer cells H1975 (5×10^6) were injected subcutaneously in the flank of female CD-1 nude mice, and treatment was initiated once the tumors reached a volume of 100 mm^3. Compound **2** was orally administered at doses of 50 and 100 mg kg^{-1} for five days per week for three weeks, whereas paclitaxel was injected by IV once a week at the optimal dose of 25 mg kg^{-1}. For the combined treatment, paclitaxel was administered by IV at day 1, 8, and 15, whereas inhibitor **2** was dosed orally from day 2 to 5, day 9 to 12, and day 16 to 19.

As reported in Figure 6, the administration of both 50 and 100 mg kg^{-1} doses of enantiomer **2** as well as the optimal dose of paclitaxel strongly decreased tumor growth with a T/C of 0.3, 0.1, and 0.18, respectively (Table 4). Interestingly, the combined treatment at the 50 mg kg^{-1} dose of enantiomer **2** and the optimal dose of paclitaxel resulted in a significant enhancement in antitumor activity (T/C of 0.05 vs. 0.3 and 0.18). Importantly, the combined treatment of the 100 mg kg^{-1} dose of enantiomer **2** and the optimal dose of paclitaxel led to an almost complete disappearance of the tumors with a T/C of 0.02. Moreover, the combined treatment of enantiomer **2** and paclitaxel was well tolerated and no significant loss of body weight was observed after three weeks of dosing.

Table 4. Tumor weight change ratio treated versus control (T/C) of single agent and combined treatment of paclitaxel and enantiomer **2**.

Compound	Dose [mg kg^{-1}]	T/C
enantiomer **2**	50	0.3
enantiomer **2**	100	0.1
paclitaxel	25	0.18
paclitaxel and enantiomer **2**	25 and 50	0.05
paclitaxel and enantiomer **2**	25 and 100	0.02

Conclusions

In conclusion, a method was developed to resolve the enantiomers of racemate **1**. Once obtained, the Hsp90 inhibitory activity of the enantiomers as well as their antiproliferative effects were investigated in comparison with those of racemic compound **1**. Enantiomer **2** was found to be a potent Hsp90 inhibitor in enzyme and cell-based assays. Enantiomer **2** had good ADME characteristics and a high oral bioavailability in mice pharmacokinetic studies. In addition, the compound demonstrated excellent antitumor activity in two different human cancer xenograft models as a single agent. Enantiomer **2** also demonstrated a synergistic effect in combination with paclitaxel in a NSCL xenograft model. We can therefore conclude that all the data obtained are supportive of the therapeutic potential of (*S*)-**2** in the treatment of cancer.

Experimental Section

Chemistry: General methods

Unless otherwise indicated, all the starting reagents and solvents (HPLC purity) were commercially available and were used without any further purification. The reactions were monitored by thin-layer chromatography (TLC) by using Merck plates 0.2 mm (60F-254) and spotting the reaction products with UV light at 254 nm. Flash chromatography purifications were performed with Merck silica gel 60 (0.04–0.063 mm). ^{1}H NMR spectra were recorded with a Bruker 300 MHz spectrometer, and ^{13}C NMR spectra were recorded with a Varian 500 MHz spectrometer. Splitting patterns describe apparent multiplicities and are designated as s (singlet), d (doublet), t (triplet), q (quartet), quint. (quintet), sext. (sextet), m (multiplet), and br. s (broad signal). HPLC–MS analyses were recorded by using one of the following methods.

Method 1: Waters Acquity UPLC, Micromass ZQ 2000 single quadrupole (Waters). Column: Phenomenex Kinetex UPLC C_{18} (50× 2.1 mm, 1.7 μm). Mobile phase: phase A: $H_2O/CH_3CN = 95:5 + 0.1\%$ trifluoroacetic acid (TFA); phase B: $H_2O/CH_3CN = 5:95 + 0.1\%$ TFA; flow rate: 0.5 mL min^{-1}. Detection: UV (diode array) among 210 e 400 nm; ESI+; full scan from $m/z = 100$ to 2000. Gradient: 0–0.3 (A: 95%, B: 5%), 0.3–1.5 (A: 0%, B: 100%), 1.5–2.0 (A: 0%, B: 100%), 2.0–2.4 min (A: 95%, B: 5%).

Method 2: Waters Acquity HPLC, Micromass ZQ 2000 Single quadrupole (Waters). Column: Acquity Atlantis C_{18} (50×2.1 mm, 3 μm). Mobile phase: phase A: $H_2O + 0.1\%$ TFA; phase B: $CH_3CN + 0.1\%$ TFA; flow rate: 0.3 mL min^{-1}. Detection: UV at 254 nm or base peak

© 2014 Wiley-VCH Verlag GmbH & Co. KGaA, Weinheim

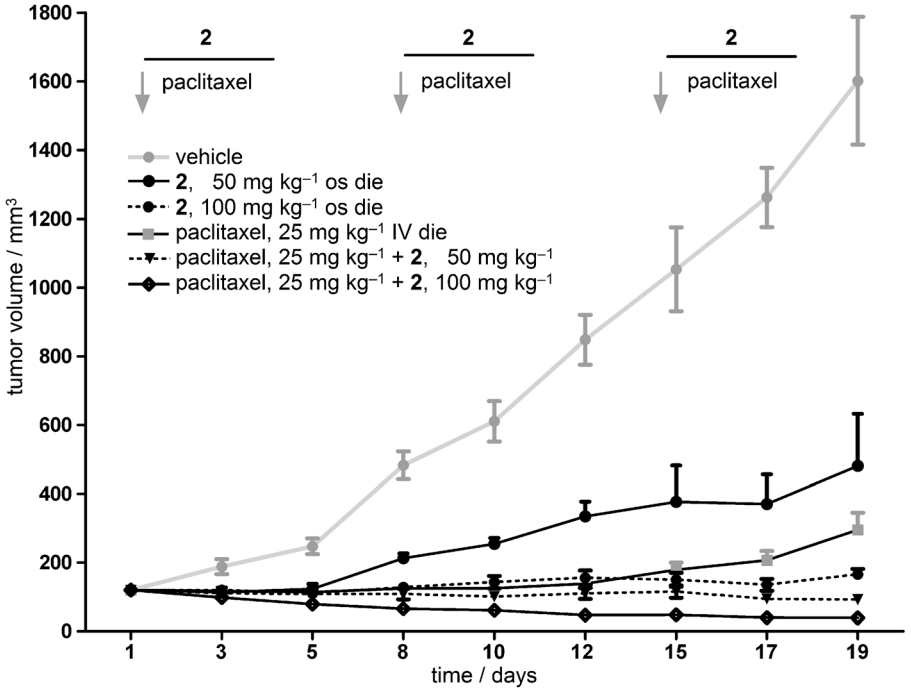

Figure 6. Antitumor activity of **2** and paclitaxel against NCI-H1975 human tumor xenografts implanted in mice, expressed as the mean tumor volume (expressed as mm^3) ± SEM.

intensity (BPI) with ESI+ at 3.2 KV, 25 V, 350 °C. Gradient: 0–0.2 (A: 95%, B: 5%), 0.2–5.0 (A: 0%, B: 100%), 5.0–6.0 (A: 0%, B: 100%), 6.0–6.1 (A: 95%, B: 5%), 6.1–7.0 min (A: 95%, B: 5%).

Method 3: (Chiral Column) Waters Alliance HPLC. Column: Chiralcel OD-H (150×4.6 mm, 5 μm). Mobile phase: phase A: *n*-hexane + 0.1% TEA; phase B: *i*PrOH + 0.1% TEA; flow rate: 0.4 mL min^{-1}. Detection: UV at 260 nm. Isocratic gradient: A: 45%, B: 55% for 25 min.

Care and husbandry of animals were in conformity with the institutional guidelines in compliance with the Italian Law (D. L.vo 116/92).

Enantiomer separation by chiral chromatography: Compound **1** was solubilized in methanol/2-propanol = 2:1 v/v (≈2 mg mL^{-1}). Enantiomeric separation was achieved by using a chiral column (Daicel Chiralpak AD Semi-preparative 250×20 mm i.d., 10 μm) and an isocratic mobile phase consisting of 75% heptane/25% 2-propanol (0.1% triethylamine). Separation conditions: flow rate 18 mL min^{-1}; injection volume 1000 μL (≈2 mg column loading); run time 60 min; UV detection at 261 nm. t_R ≈ 25 (enantiomer **3**), 40 min (enantiomer **2**). Owing to considerable tailing of enantiomer **3**, enantiomer **2** was recycled to achieve the desired enantiomeric purity. The enantiomers were obtained as white/cream-colored powders.

Procedures and characterization

(*E*)-2-Amino-7-[4-fluoro-2-(pyridin-3-yl)phenyl]-4-methyl-7,8-dihydroquinazolin-5(6*H*)-one *O*-acetyl oxime: Acetyl chloride (0.982 mL, 13.76 mmol) was added dropwise to a solution of (*E*)-2-amino-7-[4-fluoro-2-(pyridin-3-yl)phenyl]-4-methyl-7,8-dihydroquinazolin-5(6*H*)-one oxime (**1**; 5 g, 13.76 mmol) in dry DMF (100 mL) and TEA (2.88 mL, 20.64 mmol) maintaining the temperature in the 0–5 °C range. The reaction was stirred at room temperature overnight. Three further additions of acetyl chloride (0.3 mL, 4.22 mmol) and TEA (0.6 mL, 4.30 mmol) were made, and the reaction mixture was stirred at room temperature for 1 h between each addition. The solvent was removed under reduced pressure, and the crude material was washed with water and filtered. The solid thus obtained was washed with methanol, filtered, and dried under vacuum to obtain the desired compound as a white solid (5.18 g, 12.78 mmol, 93%). ^{1}H NMR (300 MHz, [D_6]DMSO): δ = 8.58 (dd, J = 4.7, 1.8 Hz, 1H), 8.55 (dd, J = 2.3, 0.9 Hz, 1H), 7.79 (dt, J = 7.9, 2.3 Hz, 1H), 7.71 (dd, J = 8.8, 5.9 Hz, 1H), 7.46 (ddd, J = 7.8, 4.8, 0.9 Hz, 1H), 7.33 (td, 1H), 7.13 (dd, J = 9.5, 2.8 Hz, 1H), 7.01 (s, 2H), 2.55–3.26 (m, 5H), 2.52 (br s, 3H), 2.16 ppm (s, 3H); LC–MS (ESI): *m/z*: 406 $[M+H]^+$; LC–MS: t_R = 0.98 min (method 1).

Racemate **1**[44] was obtained by functionalization of the intermediate ketone as a single isomer. Likely, steric hindrance of the methyl group at the 4-position prevented formation of one isomer, which led to a single derivative, the (*E*)-oxime.

(*S*,*E*)-2-Amino-7-[4-fluoro-2-(pyridin-3-yl)phenyl]-4-methyl-7,8-dihydroquinazolin-5(6*H*)-one oxime [≈80% enantiomeric excess (*ee*)] and (*R*,*E*)-2-amino-7-[4-fluoro-2-(pyridin-3-yl)phenyl]-4-methyl-7,8-dihydroquinazolin-5(6*H*)-one *O*-acetyl oxime (≈80% *ee*): Lipase acrylic resin from *C. antarctica* (0.3 g) was added to a solution of (*E*)-2-amino-7-[4-fluoro-2-(pyridin-3-yl)phenyl]-4-methyl-7,8-dihydroquinazolin-5(6*H*)-one *O*-acetyl oxime (0.2 g, 0.493 mmol) in THF (20 mL) and *n*BuOH (0.034 mL, 0.37 mmol). The suspension was stirred at 30 °C for 36 h. The enzyme was removed by filtration, and a mixture of CH_2Cl_2 and acetone (4:1, 200 mL) was added to the solution. The solution thus obtained was concentrated under reduced pressure, and the crude was purified by flash column chromatography (CH_2Cl_2/MeOH 99:1 to 95:5). Two fractions were obtained.

Fraction 1: (*R*,*E*)-2-Amino-7-[4-fluoro-2-(pyridin-3-yl)phenyl]-4-methyl-7,8-dihydroquinazolin-5(6*H*)-one *O*-acetyl oxime (0.073 g, 0.180 mmol, 73%) as a pale yellow solid. LC–MS (ESI): *m/z*: 406 $[M+H]^+$; LC–MS: t_R = 1.00 min (method 1); HPLC: t_R = 16.695 min, enantiomeric ratio: *S*/*R* = 7:93 (method 3).

Fraction 2: (*S*,*E*)-2-Amino-7-[4-fluoro-2-(pyridin-3-yl)phenyl]-4-methyl-7,8-dihydroquinazolin-5(6*H*)-one oxime (0.060 g, 0.165 mmol, 67%) as a white solid. LC–MS (ESI): *m/z*: 364 $[M+H]^+$; LC–MS: t_R = 0.92 min (method 1); HPLC: t_R = 10.646 min, enantiomeric ratio: *S*/*R* = 9:1 (method 3).

(*R*,*E*)-2-Amino-7-(4-fluoro-2-pyridin-3-yl-phenyl)-4-methyl-7,8-dihydro-6*H*-quinazolin-5-one oxime (enantiomer 3): Step A, method 1: (*R*,*E*)-2-Amino-7-[4-fluoro-2-(pyridin-3-yl)phenyl]-4-methyl-7,8-dihy-

© 2014 Wiley-VCH Verlag GmbH & Co. KGaA, Weinheim

droquinazolin-5(6*H*)-one *O*-acetyl oxime (*S*/*R* = 7:93; 0.073 g, 0.180 mmol) was triturated with a minimal amount of methanol. A white solid was obtained that was separated from the mother liquor by filtration. HPLC of the mother liquor: *R* > 99% (method 3). HPLC of the solid: *S*/*R* = 4:6 (method 3). The mother liquor was concentrated under reduced pressure to give (*R*,*E*)-2-amino-7-[4-fluoro-2-(pyridin-3-yl)phenyl]-4-methyl-7,8-dihydroquinazolin-5(6*H*)-one *O*-acetyl oxime (0.043 g, 0.108 mmol, 60%). LC–MS (ESI): *m*/*z*: 406 $[M+H]^+$; LC–MS: t_R = 0.98 min (method 1); HPLC: t_R = 16.09 min, enantiomeric ratio: *R* > 99% (method 3).

Step A, method 2: Lipase immobilized from *C. antarctica* (1.5 g) was added to a solution of (*E*)-2-amino-7-[4-fluoro-2-(pyridin-3-yl)-phenyl]-4-methyl-7,8-dihydroquinazolin-5(6*H*)-one *O*-acetyl oxime (*S*/*R* = 5:95; 1.26 g, 3.11 mmol) in dry THF (100 mL) and *n*BuOH (0.142 mL, 1.554 mmol). The mixture was stirred at 30 °C for 40 h. HPLC analysis on a chiral stationary phase showed an enantiomeric ratio of *S*/*R* = 1:99. The enzyme was removed by filtration, and a mixture of CH_2Cl_2 and acetone (4:1, 200 mL) was added to the filtered solution. The obtained solution was concentrated under reduced pressure. The crude was purified by silica gel flash chromatography (CH_2Cl_2 100% to CH_2Cl_2/MeOH = 98:2) to give the desired product (0.715 g, 1.764 mmol, 56.7%) as a pale yellow solid. LC–MS (ESI): *m*/*z*: 406 $[M+H]^+$; LC–MS: t_R = 0.99 min (method 1); HPLC: t_R = 16.09 min, enantiomeric ratio: *S*/*R* = 1:99 (method 3).

Step B: 1 M NaOH (3.53 mL, 3.53 mmol) was added to a solution of (*R*,*E*)-2-amino-7-[4-fluoro-2-(pyridin-3-yl)phenyl]-4-methyl-7,8-dihydroquinazolin-5(6*H*)-one *O*-acetyl oxime (0.715 g, 1.764 mmol) in MeOH (45 mL). The mixture was stirred at room temperature for 15 min. The solvent was removed under reduced pressure, and the crude material was washed with water, filtered, and dried under vacuum overnight to obtain the desired product (0.590 g, 1.624 mmol, 92%) as a white solid. $[\alpha]_D^{20} = -42.2$ (*c* = 0.74, acetic acid); ^{1}H NMR (300 MHz, [D$_6$]DMSO): δ = 10.91 (br. s, 1H), 8.57 (dd, *J* = 4.8, 1.6 Hz, 1H), 8.53 (dd, *J* = 2.3, 0.9 Hz, 1H), 7.77 (dt, *J* = 7.9, 2.1 Hz, 1H), 7.68 (dd, *J* = 8.9, 6.0 Hz, 1H), 7.45 (ddd, *J* = 7.8, 4.8, 0.9 Hz, 1H), 7.31 (td, *J* = 8.7, 2.9 Hz, 1H), 7.10 (dd, *J* = 9.7, 2.9 Hz, 1H), 6.65 (s, 2H), 3.01–3.12 (m, 1H), 2.99 (dd, *J* = 15.3, 12.0 Hz, 1H), 2.79–2.92 (m, 1H), 2.54–2.68 (m, 2H), 2.45 ppm (s, 3H); ^{13}C NMR (126 MHz, [D$_6$]DMSO): δ = 167.8, 165.9, 161.4, 160.7 (d, $^1J_{C,F}$ = 240.1 Hz), 152.6, 149.5, 149.2, 140.1 (d, $^3J_{C,F}$ = 7.5 Hz), 138.6 (d, $^4J_{C,F}$ = 2.9 Hz), 136.9, 135.8, 129.2 (d, $^3J_{C,F}$ = 8.5 Hz), 123.9, 117.1 (d, $^2J_{C,F}$ = 20.5 Hz), 115.9 (d, $^2J_{C,F}$ = 20.5 Hz), 112.5, 40.1, 33.6, 32.2, 26.8 ppm; LC–MS (ESI): *m*/*z*: 364.18 $[M+H]^+$; LC–MS: purity = 98%, t_R = 1.71 min (method 2); HPLC: t_R = 13.55 min, enantiomeric ratio: *S*/*R* = 1:99 (method 3).

(*S*,*E*)-2-Amino-7-[4-fluoro-2-(pyridin-3-yl)phenyl]-4-methyl-7,8-dihydro-6*H*-quinazolin-5-one oxime (enantiomer **2**): Step A: Acetyl chloride (0.357 mL, 5.00 mmol) was added to a solution of (*S*,*E*)-2-amino-7-[4-fluoro-2-(pyridin-3-yl)phenyl]-4-methyl-7,8-dihydroquinazolin-5(6*H*)-one oxime (*S*/*R* = 9:1; 1.397 g, 3.84 mmol) in dry DMF (20 mL) and TEA (0.804 mL, 5.77 mmol) maintaining the temperature in the 0–5 °C range. The mixture was stirred at room temperature. After 1 h, additional aliquots of acetyl chloride (0.273 mL, 3.84 mmol) and TEA (0.536 mL, 3.84 mmol) were added, and the mixture was stirred at room temperature overnight. The solvent was removed, and the crude material was washed with water, filtered, and dried under vacuum.

Method 1: The product thus obtained was triturated with a minimal amount of methanol. A white solid was obtained that was separated from the mother liquor by filtration. HPLC of the mother liquor: *S* > 98% (method 3). HPLC of the solid: *S*/*R* = 63:37 (method 3). The mother liquor were concentrated under reduced pressure to give (*S*,*E*)-2-amino-7-[4-fluoro-2-(pyridin-3-yl)phenyl]-4-methyl-7,8-dihydroquinazolin-5(6*H*)-one *O*-acetyl oxime (0.940 g, 2.319 mmol, 60%). LC–MS (ESI): *m*/*z*: 406 $[M+H]^+$; LC–MS: t_R = 0.98 min (method 1); HPLC: t_R = 15.919 min, enantiomeric ratio: *S* > 98% (method 3).

Method 2: Lipase immobilized from *C. antarctica* (0.8 g) was added to a solution of (*E*)-2-amino-7-[4-fluoro-2-(pyridin-3-yl)phenyl]-4-methyl-7,8-dihydroquinazolin-5(6*H*)-one *O*-acetyl oxime (*S*/*R* = 9:1; 0.433 g, 1.069 mmol) in dry THF (50 mL) and *n*BuOH (0.093 mL, 1.018 mmol). The mixture was stirred at 30 °C for two days. HPLC analysis on a chiral stationary phase showed an enantiomeric ratio of *S*/*R* = 99:1. The enzyme was removed by filtration, and a mixture of CH_2Cl_2 and acetone (4:1, 100 mL) was added to the filtered solution. The obtained solution was concentrated under reduced pressure. The crude material was purified by silica gel flash chromatography (CH_2Cl_2 100% to CH_2Cl_2/MeOH = 98:2) to give the desired product (0.202 g, 1.764 mmol, 52%) as a white solid. LC–MS (ESI): *m*/*z*: 406 $[M+H]^+$; LC–MS: t_R = 0.99 min (method 1); HPLC: t_R = 16.09 min, enantiomeric ratio: *S*/*R* = 99:1 (method 3).

Step B: 1 M NaOH (10 mL, 10 mmol) was added to a solution of (*S*,*E*)-2-amino-7-[4-fluoro-2-(pyridin-3-yl)phenyl]-4-methyl-7,8-dihydroquinazolin-5(6*H*)-one *O*-acetyl oxime (*S* > 98%; 0.940 g, 2.319 mmol) in MeOH (60 mL). The mixture was stirred at room temperature for 15 min. The solvent was removed under reduced pressure, and the crude material was washed with water, filtered, and dried under vacuum to give (*S*,*E*)-2-amino-7-[4-fluoro-2-(pyridin-3-yl)phenyl]-4-methyl-7,8-dihydroquinazolin-5(6*H*)-one oxime (0.710 g, 1.954 mmol, 84%) as a white solid: $[\alpha]_D^{20} = +39.6$ (*c* = 0.80, acetic acid); ^{1}H NMR (300 MHz, [D$_6$]DMSO): δ = 10.91 (br. s, 1H), 8.57 (dd, *J* = 4.8, 1.6 Hz, 1H), 8.53 (dd, *J* = 2.3, 0.9 Hz, 1H), 7.77 (dt, *J* = 7.9, 2.1 Hz, 1H), 7.68 (dd, *J* = 8.9, 6.0 Hz, 1H), 7.45 (ddd, *J* = 7.8, 4.8, 0.9 Hz, 1H), 7.31 (td, *J* = 8.7, 2.9 Hz, 1H), 7.10 (dd, *J* = 9.7, 2.9 Hz, 1H), 6.65 (s, 2H), 3.01–3.12 (m, 1H), 2.99 (dd, *J* = 15.3, 12.0 Hz, 1H), 2.79–2.92 (m, 1H), 2.54–2.68 (m, 2H), 2.45 ppm (s, 3H); ^{13}C NMR (126 MHz, [D$_6$]DMSO): δ = 167.8, 165.9, 161.4, 160.7 (d, $^1J_{C,F}$ = 240.1 Hz), 152.6, 149.5, 149.2, 140.1 (d, $^3J_{C,F}$ = 7.5 Hz), 138.6 (d, $^4J_{C,F}$ = 2.9 Hz), 136.9, 135.8, 129.2 (d, $^3J_{C,F}$ = 8.5 Hz), 123.9, 117.1 (d, $^2J_{C,F}$ = 20.5 Hz), 115.9 (d, $^2J_{C,F}$ = 20.5 Hz), 112.5, 40.1, 33.6, 32.2, 26.8 ppm; LC–MS (ESI): *m*/*z*: 364.08 $[M+H]^+$; LC–MS: purity = 99%, t_R = 1.71 min (method 2); HPLC: t_R = 10.83 min, enantiomeric ratio: *S*/*R* = 98:2 (method 3).

Biological assays

Hsp90 inhibitory activity: Hsp90 inhibitory activity was determined as described by Schilb et al. and Kim et al.[56,57] A Tamra–geldanamicin ligand was used as a fluorescent tracer for the Hsp90 ATPase domain. Its displacement by small-molecule inhibitors was measured by fluorescence changes.

Cell growth assay: The antiproliferative effect of the compounds was evaluated in A549 (non-small-cell lung cancer) and in HCT-116 (human colon cancer) tumor cell lines with the CellTiter-Glo Luminescent Cell Viability Assay (Promega, Madison, WI) according to the manufacturer's instructions. A549 and HCT-116 cells, in exponential growth, were incubated for 72 h at different concentrations of the inhibitors. Then, the CellTiter-Glo reagent (1 equiv) was added, the solution was mixed for 2 min to induce cell lysis, and the luminescence was recorded after an additional 10 min. The IC_{50} was calculated by using GraphPad Software.

© 2014 Wiley-VCH Verlag GmbH & Co. KGaA, Weinheim

Client protein degradation: Cells both from in vitro and in vivo experiments were lysed in lysis buffer composed of 50 mM Tris●HCl, pH 6.8, 2% SDS, and 10% glycerol. Equal amounts of protein were separated by 10% SDS-PAGE and transferred onto a nitrocellulose membrane. The membranes were incubated with 5% milk in TBST [20 mM Tris●HCl (pH 7.5), 500 mM NaCl, and 0.5% Tween 20] at room temperature for 1 h and probed with primary antibodies in 5% nonfat dried milk in TBST overnight at 4 °C. After washing three times with TBST for 5 min, the membrane was incubated with secondary anti-rabbit or anti-mouse antibody for 1 h at room temperature and visualized by enhanced chemiluminescence detection (Amersham, Bioscience Little Chalfont Buckinghamshire HP7 9NA England).

For the experiments, the following antibodies were used: Hsp70 (Hsp72) Monoclonal Antibody (C92F3A-5) form Assay Design-Stressgen (Ann Arbor USA) used at 1:1000 dilution in TBST overnight at 4 °C. Raf-1 Rabbit antibody (C-12) from Santa Cruz Biotechnologies Inc. (Dallas, TX, USA) used at 1:200 dilution in TBST overnight at 4 °C.

Microsomal stability assay: By adaptation of the protocols described by Di et al.,[58] the compounds at 1 μM were pre-incubated for 10 min at 37 °C in potassium phosphate buffer (pH 7.4) together with 0.5 mg mL^{-1} mouse or human hepatic microsomes (Xenotech, Kansas City). The cofactor mixture comprising NADP, G6P, and G6P-DH was added, and aliquots were taken after 0 and 30 min. Samples were analyzed with an Acquity UPLC, coupled with a sample organizer, and interfaced with a triple quadrupole Premiere XE (Waters, Milford, MA, USA). Mobile phases consisted of a phase A [0.1% formic acid in a mixture of water and acetonitrile (95:5 v/v)] and phase B [0.1% formic acid in a mixture of water and acetonitrile (5:95 v/v)]. Separations were achieved at 40 °C with Acquity BEH C_{18} columns (50 mm × 2.1 mm × 1.7 μm with a flow rate of 0.45 mL min^{-1} or 50 mm × 1 mm × 1.7 μm with a flow rate of 0.2 mL min^{-1}). The column was conditioned with 2% of phase B for 0.2 min, then brought to 100% of phase B within 0.01 min and maintained under these conditions for 1.3 min. The operating parameters of the mass spectrometer were set as follows: capillary voltage 3.4 kV, source temperature 115 °C, desolvation temperature 450 °C, desolvation gas flow 900 L h^{-1}, cell pressure 0.33 Pa. Cone voltage and collision energy were optimized for each compound. LC–MS/MS analyses were performed by using a positive electrospray ionization (ESI+) interface in MRM (multiple reaction monitoring) mode with verapamil as internal standard. The percentage of the compound remaining after a 30 min incubation period was calculated according to Equation (1):

$$\text{compound remaining} = \frac{\text{area at time 30 min}}{\text{area at time 0 min}} \times 100\,\% \quad (1)$$

Plasma protein binding: Compounds at a final concentration of 5 μM were incubated in mouse plasma at 37 °C for 1 h. Each sample (300 μL) was then transferred to a Centrifree vial (Millipore, Billerica, MA, USA) and centrifuged at 2700 rpm (*g* value) at 20 °C for 25 min. The filtrated portion and the initial plasma solution (40 μL) were then diluted/extracted with a CH_3CN/MeOH mixture (1:1, 160 μL) and centrifuged at 13000 rpm (*g* value) for 10 min. The solutions were analyzed by LC–MS/MS by using an ESI+ interface in multiple reaction monitoring (MRM) mode. Nonspecific binding (NSB) was determined by transferring a spiked buffer solution (300 μL) to a Centrifree vial. After centrifugation at 2700 rpm (*g* value) at 20 °C for 25 min, the filtrated portion and the initial buffer solution (40 μL) were then diluted with a CH_3CN/MeOH mixture (1:1, 160 μL) and analyzed by LC–MS/MS by using an ESI+ interface in MRM mode. The percentage of compound bound to the plasma protein (PPB) was determined according to Equation (2), in which f_u is given by Equation (3), and NSB is given by Equation (4):

$$\text{PPB} = (1 - f_u) \times 100 \quad (2)$$

$$f_u = \frac{\text{area}_{\text{filtrate}} \times (1 + \text{NSB})}{\text{area}_{\text{total}}} \quad (3)$$

$$\text{NSB} = 1 - \left(\frac{\text{area}_{\text{filtrate in buffer}}}{\text{area}_{\text{total in buffer}}}\right) \quad (4)$$

in which $\text{area}_{\text{total}}$ and $\text{area}_{\text{total in buffer}}$ refer to the samples of the test compound in a mixture composed of the initial plasma solution or buffer solution (40 μL) diluted with CH_3CN/MeOH (1:1, 160 μL) and then centrifuged.

Cytochrome P450 inhibition: Experiments were performed by adapting protocols described previously[59,60] and according to the manufacturer's instructions (BD Biosciences, Franklin Lakes, NJ, USA). The compounds were dissolved in a 96-well plate at 1 μM final concentration in potassium phosphate buffer (pH 7.4) containing an NADPH regenerating system. For all enzyme/substrate pairs, the final cofactor concentration was 1.3 mM $NADP^+$, 3.3 mM glucose-6-phosphate, and 0.4 U mL^{-1} glucose-6-phosphate dehydrogenase. The reaction was initiated by the addition of specific isoenzymes (Supersomes, Gentest) and substrates at 37 °C. Furafylline (for CYP1A2, 100 μM), sulfaphenazole (for CYP2C9, 10 μM), tranylcypromine (for CYP2C19, 500 μM), quinidine (for CYP2D6, 0.5 μM), and ketoconazole (for CYP3A4, 1.66 μM) were employed as control inhibitors in one-third serial dilution. Incubations were performed for 15 [0.5 pmol CYP1A2, 5 μM 3-cyano-7-ethoxycoumarin (CEC)], 30 {0.5 pmol CYP2C19, 25 μM CEC; 1 pmol CYP3A4, 50 μM 7-benzyloxy-4-(trifluoromethyl)coumarin; 1.5 pmol CYP2D6, 1.5 μM 3-[2-(*N*,*N*-diethyl-*N*-methylamino)ethyl]-7-methoxy-4-methylcoumarin}, or 45 min [1 pmol CYP2C9, 75 μM 7-methoxy-4-(trifluoromethyl)-coumarin]. The reaction was then quenched by adding a mixture containing 80% CH_3CN and 20% Tris base (0.5 M, 75 μL), and the plates were read by using a fluorimeter at the appropriate emission/excitation wavelengths.[60] The percentage of inhibition was calculated relative to the enzyme samples without inhibitors.

In vivo pharmacokinetic studies: Pharmacokinetic experiments were performed by using four-week-old male nude CD-1 mice (Charles River Laboratories, Calco, Italy). Animals were quarantined for approximately one week prior to the study. They were housed under standard conditions and had free access to water and standard laboratory rodent diet.

Compound **2** was dissolved in a mixture of stoichiometric 0.1 N HCl and 0.9% NaCl at a concentration of 1 mg mL^{-1} for the IV administration or stoichiometric 0.1 N HCl in water for the oral dose at a concentration of 3 mg mL^{-1}. Compound **3** was dissolved in a mixture of stoichiometric 0.1 N HCl, 3% DMSO, and 0.9% NaCl at a concentration of 1 mg mL^{-1} for the IV administration or stoichiometric 0.1 N HCl in water for the oral dose at a concentration of 3 mg mL^{-1}. Each experimental group contained 27 animals. The compounds were administered to mice either by IV or oral route, and blood samples were collected at different time points after dosing. Plasma was separated immediately after blood sampling by centrifugation, plasma proteins were precipitated by using Sirocco filtration plates, and the plasma samples were kept frozen (−80 °C) until submission to LC–MS/MS analysis. Sample analysis was performed with an Acquity UPLC by using an Acquity HSS T3 column (50 mm × 2.1 mm × 1.8 μm), coupled with a sample organizer and interfaced to a triple quadrupole Premiere XE (Waters, Mil-

© 2014 Wiley-VCH Verlag GmbH & Co. KGaA, Weinheim

ford, MA). The mass spectrometer was operated by using ESI with a capillary voltage of 3–4 kV, cone voltage of 25–52 V, source temperature of 115–120 °C, desolvation gas flow of 800 L h^{-1}, and desolvation temperature of 450–480 °C. Collision energy was optimized for each compound. LC–MS/MS analyses were performed by using ESI+ in MRM mode.

Plasma concentrations of compounds **2** and **3** were extrapolated on eight-point calibration curves (2.5–1000 ng mL^{-1}). Quality control (QC) samples of the test compound at three different concentrations (high, medium, and low) were considered for acceptance of the analytical runs with an accuracy within ±15% except at the lowest limit of quantification of 5 ng mL^{-1} for which ±20% was accepted. Pharmacokinetic parameters were calculated by a noncompartmental method by using WinNonLin 5.1 software (Pharsight, Mountain View, CA, USA).

In vivo xenograft study (HCT-116 xenograft and NSCL xenograft): For in vivo antitumor efficacy studies, 5 million human cancer cells (HCT-116 or NCI-H1975) were injected subcutaneously in the flank of female CD-1 nude mice (aged six weeks, Charles River Laboratories, Wilmington, MA). Tumors were allowed to grow until volumes of ~100 mm^3 were reached. Mice bearing a tumor xenograft were randomized into treated and control groups of seven animals per group. Hsp90 inhibitors were dissolved in a vehicle corresponding to a mixture of stoichiometric 0.1 N HCl, 0.5% methylcellulose, and 1% Tween 80 in water. Paclitaxel (LC laboratories Woburn, USA) was dissolved in a mixture containing 50% Cremophor EL (Sigma–Aldrich, Steinheim, Germany) and 50% ethanol and further diluted 10-fold in a solution of 0.9% NaCl.

In the HCT-116 xenograft experiment, Hsp90 inhibitors were administered five days per week for 16 days. In the NCI H-1975 experiment, compound **2** was orally administered at the suboptimal and optimal doses of 50 and 100 mg kg^{-1} for five days per week for three weeks, whereas paclitaxel was injected by IV once a week at the optimal dose of 25 mg kg^{-1}. For the combined treatment, paclitaxel was IV administered at day 1, 8, and 15, whereas inhibitor **2** was dosed from day 2 to 5, day 9 to 12, and day 16 to 19.

Acknowledgements

The authors thank Florian Thaler for his contribution to the preparation of this manuscript.

Keywords: antitumor agents · chiral resolution · enantiomers · Hsp90 · oximes

[1] A. Kamal, L. Thao, J. Sensintaffar, L. Zhang, M. F. Boehm, L. C. Fritz, F. J. Burrows, *Nature* **2003**, *425*, 407 – 410.
[2] L. H. Pearl, C. Prodromou, *Adv. Protein Chem.* **2001**, *59*, 157 – 186.
[3] S. Chaudhury, T. R. Welch, B. S. Blagg, *ChemMedChem* **2006**, *1*, 1331 – 1340.
[4] K. Richter, J. Buchner, *J. Cell. Physiol.* **2001**, *188*, 281 – 290.
[5] J. Trepel, M. Mollapour, G. Giaccone, L. Neckers, *Nat. Rev. Cancer* **2010**, *10*, 537 – 549.
[6] M. Taipale, D. F. Jarosz, S. Lindquist, *Nat. Rev. Mol. Cell Biol.* **2010**, *11*, 515 – 528.
[7] K. Sidera, E. Patsavoudi, *Recent Pat. Anti-Cancer Drug Discovery* **2014**, *9*, 1 – 20.
[8] T. Zhang, A. Hamza, X. Cao, B. Wang, S. Yu, C. G. Zhan, D. Sun, *Mol. Cancer Ther.* **2008**, *7*, 162 – 170.
[9] K. Kawakami, M. Kohno, T. Horibe (Kyoto University), Int. PCT Pub. No. WO/2010/055929 A1, **2010**.
[10] D. C. Altieri, J. Plescia, W. Saltz (University of Massachusetts), Int. PCT Pub. No. WO/2006/014744 A3, **2006**.
[11] V. C. Ardi, L. D. Alexander, V. A. Johnson, S. R. McAlpine, *ACS Chem. Biol.* **2011**, *6*, 1357 – 1366.
[12] B. Becker, G. Multhoff, B. Farkas, P. J. Wild, M. Landthaler, W. Stolz, T. Vogt, *Exp. Dermatol.* **2004**, *13*, 27 – 32.
[13] E. Pick, Y. Kluger, J. M. Giltnane, C. Moeder, R. L. Camp, D. L. Rimm, H. M. Kluger, *Cancer Res.* **2007**, *67*, 2932 – 2937.
[14] F. Zagouri, A. Nonni, T. N. Sergentanis, C. A. Papadimitriou, N. V. Michalopoulos, A. C. Lazaris, E. Patsouris, G. C. Zografos, *BMC Cancer* **2008**, *8*, 312.
[15] C. F. Li, W. W. Huang, J. M. Wu, S. C. Yu, T. H. Hu, Y. H. Uen, Y. F. Tian, C. N. Lin, D. Lu, F. M. Fang, H. Y. Huang, *Clin. Cancer Res.* **2008**, *14*, 7822 – 7831.
[16] P. Flandrin, D. Guyotat, A. Duval, J. Cornillon, E. Tavernier, N. Nadal, L. Campos, *Cell Stress Chaperones* **2008**, *13*, 357 – 364.
[17] X. Wu, A. Wanders, P. Wardega, B. Tinge, L. Gedda, S. Bergstrom, L. Sooman, J. Gullbo, M. Bergqvist, P. Hesselius, J. Lennartsson, S. Ekman, *Br. J. Cancer* **2009**, *100*, 334 – 343.
[18] M. C. Diehl, M. O. Idowu, K. Kimmelshue, T. P. York, L. W. Elmore, S. E. Holt, *Cancer Biol. Ther.* **2009**, *8*, 1952 – 1961.
[19] G. H. Kang, E. J. Lee, K. T. Jang, K. M. Kim, C. K. Park, C. S. Lee, D. Y. Kang, S. H. Lee, T. S. Sohn, S. Kim, *Histopathology* **2010**, *56*, 694 – 701.
[20] D. S. Hong, U. Banerji, B. Tavana, G. C. George, J. Aaron, R. Kurzrock, *Cancer Treat. Rev.* **2013**, *39*, 375 – 387.
[21] R. B. Den, B. Lu, *Ther. Adv. Med. Oncol.* **2012**, *4*, 211 – 218.
[22] L. Neckers, P. Workman, *Clin Cancer Res.* **2012**, *18*, 64 – 76.
[23] J. Travers, S. Sharp, P. Workman, *Drug Discovery Today* **2012**, *17*, 242 – 252.
[24] A. Donnelly, B. S. Blagg, *Curr. Med. Chem.* **2008**, *15*, 2702 – 2717.
[25] L. Neckers, J. B. Trepel, *Clin Cancer Res.* **2014**, *20*, 275 – 277.
[26] K. Jhaveri, T. Taldone, S. Modi, G. Chiosis, *Biochim. Biophys. Acta Mol. Cell Res.* **2012**, *1823*, 742 – 755.
[27] J. Bussenius, C. M. Blazey, N. Aay, N. K. Anand, A. Arcalas, T. Baik, O. J. Bowles, C. A. Buhr, S. Costanzo, J. K. Curtis, S. C. DeFina, L. Dubenko, T. S. Heuer, P. Huang, C. Jaeger, A. Joshi, A. R. Kennedy, A. I. Kim, K. Lara, J. Lee, J. Li, J. C. Lougheed, S. Ma, S. Malek, J. C. Manalo, J. F. Martini, G. McGrath, M. Nicoll, J. M. Nuss, M. Pack, C. J. Peto, T. H. Tsang, L. Wang, S. W. Womble, M. Yakes, W. Zhang, K. D. Rice, *Bioorg. Med. Chem. Lett.* **2012**, *22*, 5396 – 5404.
[28] R. Bao, C. J. Lai, H. Qu, D. Wang, L. Yin, B. Zifcak, R. Atoyan, J. Wang, M. Samson, J. Forrester, S. DellaRocca, G. X. Xu, X. Tao, H. X. Zhai, X. Cai, C. Qian, *Clin. Cancer Res.* **2009**, *15*, 4046 – 4057.
[29] S. H. Kim, A. Bajji, R. Tangallapally, B. Markovitz, R. Trovato, M. Shenderovich, V. Baichwal, P. Bartel, D. Cimbora, R. McKinnon, R. Robinson, D. Papac, D. Wettstein, R. Carlson, K. M. Yager, *J. Med. Chem.* **2012**, *55*, 7480 – 7501.
[30] K. H. Huang, J. M. Veal, R. P. Fadden, J. W. Rice, J. Eaves, J. P. Strachan, A. F. Barabasz, B. E. Foley, T. E. Barta, W. Ma, M. A. Silinski, M. Hu, J. M. Partridge, A. Scott, L. G. DuBois, T. Freed, P. M. Steed, A. J. Ommen, E. D. Smith, P. F. Hughes, A. R. Woodward, G. J. Hanson, W. S. McCall, C. J. Markworth, L. Hinkley, M. Jenks, L. Geng, M. Lewis, J. Otto, B. Pronk, K. Verleysen, S. E. Hall, *J. Med. Chem.* **2009**, *52*, 4288 – 4305.
[31] S. R. Kasibhatla, K. Hong, M. A. Biamonte, D. J. Busch, P. L. Karjian, J. L. Sensintaffar, A. Kamal, R. E. Lough, J. Brekken, K. Lundgren, R. Grecko, G. A. Timony, Y. Ran, R. Mansfield, L. C. Fritz, E. Ulm, F. J. Burrows, M. F. Boehm, *J. Med. Chem.* **2007**, *50*, 2767 – 2778.
[32] D. L. Menezes, P. Taverna, M. R. Jensen, T. Abrams, D. Stuart, G. K. Yu, D. Duhl, T. Machajewski, W. R. Sellers, N. K. Pryer, Z. Gao, *Mol. Cancer Ther.* **2012**, *11*, 730 – 739.
[33] P. A. Brough, W. Aherne, X. Barril, J. Borgognoni, K. Boxall, J. E. Cansfield, K. M. Cheung, I. Collins, N. G. Davies, M. J. Drysdale, B. Dymock, S. A. Eccles, H. Finch, A. Fink, A. Hayes, R. Howes, R. E. Hubbard, K. James, A. M. Jordan, A. Lockie, V. Martins, A. Massey, T. P. Matthews, E. McDonald, C. J. Northfield, L. H. Pearl, C. Prodromou, S. Ray, F. I. Raynaud, S. D. Roughley, S. Y. Sharp, A. Surgenor, D. L. Walmsley, P. Webb, M. Wood, P. Workman, L. Wright, *J. Med. Chem.* **2008**, *51*, 196 – 218.
[34] A. J. Woodhead, H. Angove, M. G. Carr, G. Chessari, M. Congreve, J. E. Coyle, J. Cosme, B. Graham, P. J. Day, R. Downham, L. Fazal, R. Feltell, E. Figueroa, M. Frederickson, J. Lewis, R. McMenamin, C. W. Murray, M. A. O'Brien, L. Parra, S. Patel, T. Phillips, D. C. Rees, S. Rich, D. M. Smith, G.

© 2014 Wiley-VCH Verlag GmbH & Co. KGaA, Weinheim

Trewartha, M. Vinkovic, B. Williams, A. J. Woolford, *J. Med. Chem.* **2010**, *53*, 5956 – 5969.
[35] W. Ying, Z. Du, L. Sun, K. P. Foley, D. A. Proia, R. K. Blackman, D. Zhou, T. Inoue, N. Tatsuta, J. Sang, S. Ye, J. Acquaviva, L. S. Ogawa, Y. Wada, J. Barsoum, K. Koya, *Mol. Cancer Ther.* **2012**, *11*, 475 – 484.
[36] T. Nakashima, T. Ishii, H. Tagaya, T. Seike, H. Nakagawa, Y. Kanda, S. Akinaga, S. Soga, Y. Shiotsu, *Clin. Cancer Res.* **2010**, *16*, 2792 – 2802.
[37] R. M. Immormino, Y. Kang, G. Chiosis, D. T. Gewirth, *J. Med. Chem.* **2006**, *49*, 4953 – 4960.
[38] J. P. Calvet, B. S. J. Blagg, S. V. Sundar, B. S. Magenheimer (University of Kansas), Int. PCT Pub. No. WO/2011/041593 A1, **2011**.
[39] J. D. Eskew, T. Sadikot, P. Morales, A. Duren, I. Dunwiddie, M. Swink, X. Zhang, S. Hembruff, A. Donnelly, R. A. Rajewski, B. S. Blagg, J. R. Manjarrez, R. L. Matts, J. M. Holzbeierlein, G. A. Vielhauer, *BMC Cancer* **2011**, *11*, 468.
[40] H. Zhao, B. S. J. Blagg in *Inhibitors of Molecular Chaperones as Therapeutic Agents* (Eds.: T. D. Machajewski, Z. Gao), Royal Society of Chemistry, Cambridge, **2013**, ch. 10.
[41] S. M. Cohen, R. Mukerji, A. K. Samadi, X. Zhang, H. Zhao, B. S. Blagg, M. S. Cohen, *Ann. Surg. Oncol.* **2012**, *19*, 483 – 490.
[42] R. Conde, Z. R. Belak, M. Nair, R. F. O'Carroll, N. Ovsenek, *Biochem. Cell Biol.* **2009**, *87*, 845 – 851.
[43] F. Guo, K. Rocha, P. Bali, M. Pranpat, W. Fiskus, S. Boyapalle, S. Kumaraswamy, M. Balasis, B. Greedy, E. S. Armitage, N. Lawrence, K. Bhalla, *Cancer Res.* **2005**, *65*, 10536 – 10544.
[44] J. J. Barker, O. Barker, R. Boggio, V. Chauhan, R. K. Cheng, V. Corden, S. M. Courtney, N. Edwards, V. M. Falque, F. Fusar, M. Gardiner, E. M. Hamelin, T. Hesterkamp, O. Ichihara, R. S. Jones, O. Mather, C. Mercurio, S. Minucci, C. A. Montalbetti, A. Muller, D. Patel, B. G. Phillips, M. Varasi, M. Whittaker, D. Winkler, C. J. Yarnold, *ChemMedChem* **2009**, *4*, 963 – 966.
[45] L. Neckers, *Trends Mol. Med.* **2002**, *8*, S55 – 61.
[46] R. L. Walsky, S. E. Boldt, *Curr. Drug Metab.* **2008**, *9*, 928 – 939.
[47] C.-S. Chen, C. J. Sih, *Angew. Chem. Int. Ed. Engl.* **1989**, *28*, 695 – 707; *Angew. Chem.* **1989**, *101*, 711 – 724.
[48] J.-M. Fang, C.-H. Wong, *Synlett* **1994**, 393 – 402.
[49] S. Fernández, E. Menéndez, V. Gotor, *Synthesis* **1991**, 713 – 716.
[50] A. Ghogare, G. S. Kumar, *J. Chem. Soc. Chem. Commun.* **1989**, 1533 – 1535.
[51] A. Ghogare, G. S. Kumar, *J. Chem. Soc. Chem. Commun.* **1990**, 134 – 135.
[52] R. Pulido, F. L. Ortiz, V. Gotor, *J. Chem. Soc. Perkin Trans. 1* **1992**, 2891 – 2898.
[53] R. Matusch, C. Coors, *Angew. Chem. Int. Ed. Engl.* **1989**, *28*, 626 – 627; *Angew. Chem.* **1989**, *101*, 624 – 626.
[54] R.-M. Nicoud, J.-N. Jaubert, I. Rupprecht, J. Kinkel, *Chirality* **1996**, *8*, 234 – 243.
[55] B. Davies, T. Morris, *Pharm. Res.* **1993**, *10*, 1093 – 1095.
[56] A. Schilb, V. Riou, J. Schoepfer, J. Ottl, K. Muller, P. Chene, L. M. Mayr, I. Filipuzzi, *J. Biomol. Screening* **2004**, *9*, 569 – 577.
[57] J. Kim, S. Felts, L. Llauger, H. He, H. Huezo, N. Rosen, G. Chiosis, *J. Biomol. Screening* **2004**, *9*, 375 – 381.
[58] L. Di, E. H. Kerns, N. Gao, S. Q. Li, Y. Huang, J. L. Bourassa, D. M. Huryn, *J. Pharm. Sci.* **2004**, *93*, 1537 – 1544.
[59] E. A. Dierks, K. R. Stams, H.-K. Lim, G. Cornelius, H. Zhang, S. E. Ball, *Drug Metab. Dispos.* **2001**, *29*, 23 – 29.
[60] C. L. Crespi, V. P. Miller, D. M. Stresser, *Methods Enzymol.* **2002**, *357*, 276 – 284.

Received: January 14, 2014
Published online on April 17, 2014

© 2014 Wiley-VCH Verlag GmbH & Co. KGaA, Weinheim